atoms

MDPI

Article

Absolute Double Differential Cross Sections of Bremsstrahlung Produced from 4.0 keV Electrons Incident on Free Ar Atoms

Suman Prajapati [1], Bhupendra Singh [2], Sunil Kumar [3], Bhartendu Kumar Singh [1], C. A. Quarles [4] and R. Shanker [1,*]

1 Atomic Physics Laboratory, Department of Physics, Banaras Hindu University, Varanasi 221005, India; sumanprajapati603@gmail.com (S.P.); bhartendu.k.singh@gmail.com (B.K.S.)
2 Department of Physics, Central University of Jharkhand, Ranchi 835205, Jharkhand, India; bhupendra.singh@cuj.ac.in
3 Department of Particle Physics and Astrophysics, Wiezmann Institute of Science, Rehovot 7610001, Israel; sunilphy88@gmail.com
4 Department of Particle Physics and Astronomy, Texas Christian University, Fort Worth, TX 76129, USA; c.quarles@tcu.edu
* Correspondence: shankerorama@gmail.com

Received: 17 September 2020; Accepted: 7 October 2020; Published: 12 October 2020

Abstract: New results are reported on the measurements of *absolute double differential cross sections* (DDCSs) of bremsstrahlung produced from 4.0 keV electrons incident on free Ar atoms in the angular detection range of 45°–120°. A significant reduction of the thick target bremsstrahlung (TTB) of the chamber wall and of the photon transmission windows has been achieved by modifying the experimental set-up used previously; a large reduction of TTB in the present experiments is supported by the results of our model calculations for the ratio of TTB background to the normal bremsstrahlung (NB) spectrum carried out for the employed geometry of the experimental set-up. The results of photon energy distribution measured at different angles and those of angular distributions of photons of a given energy are compared with theoretical predictions of Kissel–Quarles–Pratt (KQP) theory for ordinary bremsstrahlung and with predictions of total bremsstrahlung including polarization bremsstrahlung (PBS) of the stripping approximation (SA). A satisfactory agreement observed between experiment and predictions using SA theory for absolute DDCSs of bremsstrahlung provides evidence for an appreciable contribution of polarization bremsstrahlung at the considered impact energy of electrons on one hand, while on the other hand, it exhibits a large discrepancy (about a factor of 2) in DDCSs of bremsstrahlung photons obtained by experiment and by KQP theory for photon energy distributions at all detection angles measured in these experiments. In addition, present results of the angular dependence of photons of different energies show anisotropic distributions and they are found to be in reasonable agreement with both KQP and SA theories. The satisfactory agreement between experiment and theory for angular distributions is an indication of a significant reduction of the background produced from TTB photons.

Keywords: angular distributions; ordinary bremsstrahlung; polarization bremsstrahlung; stripping approximation; thick target bremsstrahlung

1. Introduction

The bremsstrahlung (BS) emission in collisions of a charged particle with a target atom or a molecule takes place via two mechanisms: in the first mechanism, the BS emission arises due to the deceleration of the projectile particle in the Coulomb field of the target atom or the molecule, called

ordinary bremsstrahlung (OBS). Several experimental and theoretical studies have been done in the past on the determination of BS cross sections in the frame of OBS from gaseous atoms/molecules by electron impact [1–9]. A benchmark theoretical work on OBS calculations using relativistic partial wave Born approximation is available in tabular form by Kissel–Quarles–Pratt (KQP) [10]. In several experimental studies, the comparison of BS cross sections has been made with the theory of OBS. In the second mechanism, a new type of bremsstrahlung arises as a result of the dynamic polarization of the target atom by the incident particle; basically it is the atomic electrons virtually excited from their initial states, which radiate in the polarization process. This mechanism of polarization bremsstrahlung (PBS) was first theoretically proposed by Buimistrov and Trakhtenberg [11] in which it was suggested that a dipole is induced in the target atom as a result of repulsion felt by atomic electrons due to the field of the energetic projectile electron. The relaxation of the induced atomic dipole moment results in the emission of photons of continuous energy lying in the region of X-rays. Thus, in an electron–atom collision, a continuous radiation could be emitted not only by the incoming electron, but also by the target atom. The first experimental observation of PBS was made in Xe atoms [12]. A number of reviews on PBS are available in the literature, for example, by Korol et al. [13–15]. The bremsstrahlung process has a broad range of implications in different areas of science in addition to being of interest on its own, for instance, the observation of the emission of bremsstrahlung from free-free transitions of low-energy (1.2 to 5.4 eV) electrons in Ar discharges [16]. The emission of bremsstrahlung radiation is related to the gas discharges due to runaway electrons in the atmosphere inducing lightning development in its early stages [17]. Furthermore, the visible bremsstrahlung radiation has been used to measure the effective ion charges as impurity content in fusion devices [18]. In recent years, the electron–atom bremsstrahlung process within the rigorous relativistic approach based on the partial-wave expansion of the Dirac wave functions in the external atomic field has been studied for a wide range of atoms, as well as a function of photon angles, as shown in [19,20] and references therein.

Quite a few experimental studies have been carried out to look for PBS contribution to the DDCSs of BS for incident electron energies in the range of 25–100 keV from thin films of various atomic numbers; a very useful review on this topic can be found by Quarles and Portillo [21]. Several experimental and theoretical works on continuous X-rays produced through various processes including the process of PBS in light ion–atom collisions with MeV impact energies have been carried out, for example, by Ishii and his coworkers, [22–25] and references therein. The search for the PBS contribution to the thick target yields was made and expected to be especially present at a lower energy of radiated photons. However, no clear evidence for a PBS contribution was established and the data were found to be in good agreement with the general purpose PENELOPE calculations [26]. Portillo and Quarles [27] measured the absolute DDCSs of BS from collisions of 28 keV and 50 keV electrons with Ne, Ar, Kr and Xe gaseous atoms and have found a significant enhancement over the prediction of OBS; there was a good agreement with the magnitude of the stripping approximation (SA) [28] calculations for 28 keV and 50 keV electron impacts on Kr and Xe, however, there was no evidence for the discontinuities near the absorption edges predicted by SA. The experimental results for Ar were significantly higher than those of SA prediction. For seeing the clear contribution of PBS, the main challenge is to minimize various sources of background radiations associated with the BS spectrum; the most important among these are the thick target bremsstrahlung (TTB) radiations which are produced due to the scattered electrons from the gaseous target that hit the chamber wall to produce TTB radiation. The TTB radiation is produced with greater intensity in the forward direction than in the backward direction, that is, TTB radiation is more intense when viewed at detection angles greater than 90°.

The literature survey reveals that studies of the angular dependence of the DDCSs of BS photons have been done mostly for thick targets and thin foils [29–31]. Such studies are, however, scarce for free atomic and molecular targets. The only study on the angular distributions of DDCSs of BS radiation produced by electrons of energy in the range 3–15 keV incident on Ar, Kr and Xe was done by Aydinol et al. [32]; in these studies, the observed anisotropy of the BS radiation was explained by a modified Sommerfeld formula. Recently, Yadav et al. [33] have conducted the measurements of angular and

photon energy distributions of the BS photons produced from 4.0 keV electrons incident on free Ar atoms with reasonable reduction (about a factor of 5) of TTB background. They have compared the *relative* DDCSs of BS photons with the theoretical predictions of the OBS and the SA and have concluded that further reduction of TTB background is necessary to establish the existence of PBS contribution with greater confidence. Furthermore, there has been a theoretical study of double differential cross sections of BS and PBS photons for the scattering of relativistic electrons with free Ar atoms by Astapenko [34]; this study enables the identification of different channels involved in the BS process.

In the present work, we report on the experimental and theoretical results of *absolute DDCSs* of BS radiation produced from 4.0 keV electrons incident on free Ar atoms after making a significant reduction of TTB contribution almost by a factor of 30 compared to the one obtained without TTB reduction. This has been made possible by modifying the experimental set-up that was used in our previous work [33] with respect to collimation of the BS photons generated from the electron–Ar collision reaction. In this new configuration, the BS photons generated at the collision center were monitored by a system with a long graphite collimator (30 mm) with end apertures of about 2 mm and the detectors all set to lie exactly in the line of sight of the detector; thus viewing a very small cross section area of the material of the chamber wall relevant to TTB photon contribution. This arrangement facilitated us to measure the angular and photon energy distributions of BS radiation with greater confidence. Even though the usage of this experimental configuration could reduce the TTB contribution greatly, still it was not possible to separate the contribution of PBS from ordinary bremsstrahlung explicitly. In spite of having this unfavorable situation, the DDCS results thus obtained have been put on an absolute scale by following a procedure described in Section 4. It is shown that there is much better absolute agreement between the experiment and the SA theory in comparison to the KQP predictions. This agreement provides at least one good piece of evidence for the contribution of PBS at the considered impact energy of electrons. Furthermore, our data show a good agreement between experiment and theories for the angular distributions of BS photons of different energies, indicating a significant reduction in the background generated from thick target walls. The reduction of background generated at extreme detection angles is found to be only up to a few percent. This conclusion is supported by our model calculations of the ratio of TTB background from the walls and the photon transmission windows to the normal BS spectrum for the employed geometry of the experimental set-up, as discussed in Section 3.

2. Experimental Details

The experimental set-up employed in the present work for studying the angular and photon energy distributions of BS radiation emitted from 4.0keV electrons incident on free Ar atoms is similar to the one used in our previous work of Yadav et. al. [33], except two modifications that were made, as described below.

Two modifications have been implemented for performing the present measurements, namely, (i) a Pfeiffer turbo-molecular pump (TPH-240) of 240 L/s pumping speed coupled with a two-stage Edward-8 rotary pump was used in place of an oil diffusion pump (150 L/s), (ii) the teflon cylinder (Z = 6) which was used as an inner scattering chamber in our previous set-up was removed in the present experiments. An assembly of a graphite collimator with length 30 mm, aperture diameter 2 mm and a rotatable detector platform made a combined system. This system was attached to the gas target holder and a hypodermic needle by two separate connecting rods (see, Figure 1). This arrangement allowed us to move the angular movement of the collimator and the detector in unison around the collision center for detecting the photons emitted from the collision center. In this configuration, the solid angle subtended by the detector to the chamber wall was considerably reduced, causing a relatively longer duration of the data acquisition due to reduced total photon counts on one hand, but on the other hand, a great deal of reduction of the TTB radiation almost by a factor of 30 was achieved compared to when this arrangement was not used. A schematic diagram of the modified experimental set-up is shown in Figure 1.

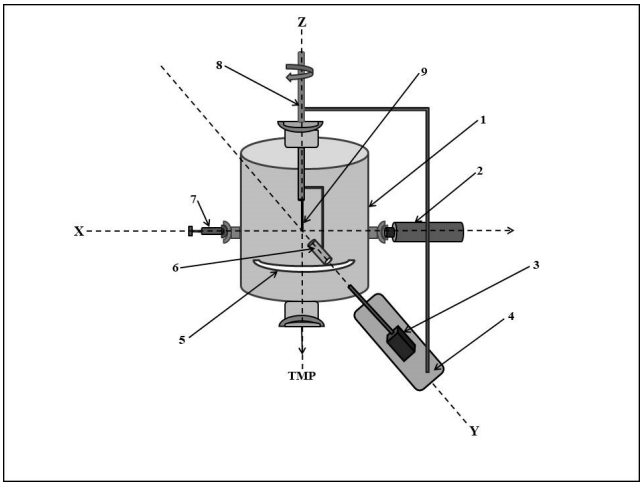

Figure 1. Schematic of the modified experimental set-up with different components marked in the figure. X-, Y- and Z-axes show the directions of electron beam, photon detection and gas flow, respectively. 1—scattering chamber, 2—electron gun, 3—Si PIN photodiode detector, 4—rotatable platform, 5—hostaphan window, 6—graphite collimator, 7—Faraday cup, 8—gas target holder, 9—hypodermic needle and TMP—turbo molecular pump. The graphite collimator, hypodermic needle and the detector move in unison and remain collinear with the collision center at all detection angles of measurements.

Briefly, a well-focused mono-energetic beam of electrons (diameter ~1–2 mm) was made to collide with free Ar gas atoms effusing from a hypodermic needle (length = 20.0 mm, diameter = 1.3 mm). The tip of the needle was kept about 2 mm above the electron beam level. The beam current was measured on a Faraday cup and integrated by using a current integrator (Ortec Model 419). The Faraday cup was biased by +32 V using a dry battery in order to suppress the secondary electrons. The beam current was kept in the range 5–6 μA during all measurements. The base pressure of the chamber without gas load was 3×10^{-7} Torr while the pressure of the chamber with gas load was kept around 5×10^{-4} Torr, ensuring the single collision condition.

BS photons emerging from the collision zone passed through a graphite collimator and a hostaphan foil window of the chamber and were detected by a Si-PIN photodiode detector (M/s Amptek Inc., Bedford, MA, USA) placed outside of the chamber at a distance of 10 mm from the hostaphan window. The detector was thermoelectrically cooled at −30 °C; the resolution of the detector was measured to be 196 eV at 5.9 keV using a Fe-55 radioactive source. An Al aperture with a diameter of 3 mm was attached to the entrance of the photon detector. The angular measurements were performed by rotating the detector mounted on a rotatable platform, as shown in Figure 1. The angular position of the detector was read on a scale affixed on the scattering chamber (angular least count = 5°). The total distance between the detector and the collision center was about 52 mm. This distance includes an air column of 10 mm between the chamber and the Al aperture. The solid angle subtended by the detector at the collision center was about 4.3×10^{-4} sr. BS spectra produced from 4.0 keV electrons incident on Ar atoms were recorded by using a computer-based multichannel analyzer (MCA-3; FAST ComTech GmbH, 1.6 GHz) in a pulse height analysis mode. The BS spectra were also recorded with *beam-on* and *gas-off* conditions for all angles; these measurements were needed for background subtraction during the data analysis. The background count was found to be insignificant (<1 count/s). The average gas count rate of photons in all measurements was in the range of 50–60 counts/s. For obtaining reasonable statistics of the data, the acquisition time for all measurements ranged from 3 h to 5 h.

3. Background Processes in Gas BS Spectrum

The spectra of electron bremsstrahlung produced from gaseous targets are found to comprise, in general, an ordinary bremsstrahlung (OBS) and the polarization bremsstrahlung (PBS) spectra. In addition to these spectra, the gas BS spectrum contains an inherent contribution of a thick target bremsstrahlung (TTB) background which is produced from scattered electrons from the gaseous target while hitting the chamber wall and the photon transmission windows. Furthermore, there are other background radiations that may be present; that is, the background photons produced due to Rayleigh and Compton scattering from the gaseous target by beam photons. The beam photons are produced from the interaction of the electron beam with beam line collimators. The background radiation caused by Rayleigh and Compton scatterings cannot be measured in the beam-on and the target gas-off runs. The photon counts seen by the detector in the beam line produced by the electron beam interaction with beam collimators can be minimized to a very small magnitude; for example, by using a long graphite collimator in a passage of photons from the target to the detector (as is the case for the present experiments). Such a background photon count in the present experiments for all measured detection angles was found to be <1 count/s when there was no gas present in the chamber. A significant contribution of the TTB background particularly at large detection angles is of paramount importance in the gas target BS experiments. Reduction of TTB background from scattered electrons with the chamber wall and the photon transmission windows has been theoretically estimated following a model given by Quarles [35] and Semann and Quarles [36] for our employed experimental geometry. In this model calculation, appropriate values of elastic scattering of 4.0 keV electrons with Ar free atoms have been used. In order to determine the magnitude of the background effects, the ratio of TTB background spectrum from the chamber wall and the photon transmission window (hostaphan) to the normal gas BS spectrum as a function of detection angle for photon energies of 2.4 keV and 3.6 keV has been calculated with the graphite collimator in place. The results are plotted in Figure 2.

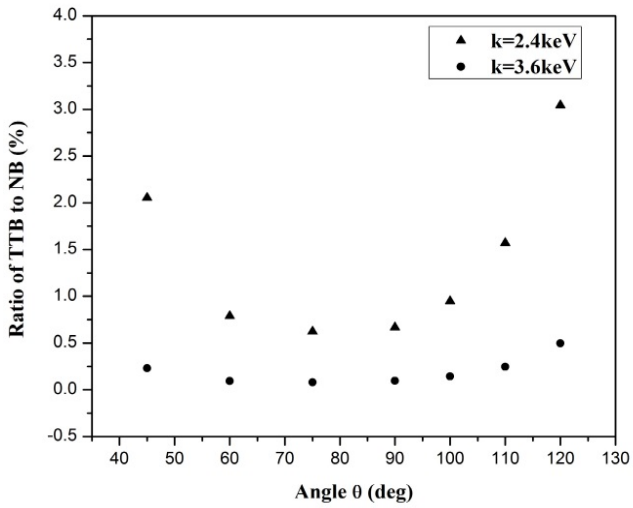

Figure 2. Model calculations of the ratio of total thick target bremsstrahlung TTB background to the normal gas bremsstrahlung BS (NB) emitted from 4.0 keV electron collisions with free argon atoms as a function of detection angle (θ) for photon energies of 2.4 keV and 3.6 keV.

From the plot shown in Figure 2, we see that the background is highly negligible at the highest photon energy. While larger at the lowest photon energy, it is still small except at the extreme angles where the background could be 2 to 3% of the bremsstrahlung rate. So, a reduction in the rate based on this analysis seems reasonable. In view of this result, we can conservatively assume an error in the background correction of about twice the ratio obtained for 2.4 keV photons at extreme angles. Thus, the error can be increased in this case by a few percent to account for uncertainty in the solid angles and the effects of electron scattering from other areas of the gas or uncertainty in the gas target distribution.

Furthermore, from Figure 3, it is seen that the ratio of total TTB background from wall and window to the normal gas BS spectrum *with collimator in place* for 2.4 keV photons detected at 120° is about 0.03 while the same ratio calculated for the case when the *collimator is not used* is found to be about 5.13. That is, the TTB background is almost 170 times smaller than the normal gas BS when the collimator is in place, suggesting that the TTB background present in the current experiments is very small or negligible when compared to the previous experimental results where such a collimator was not used.

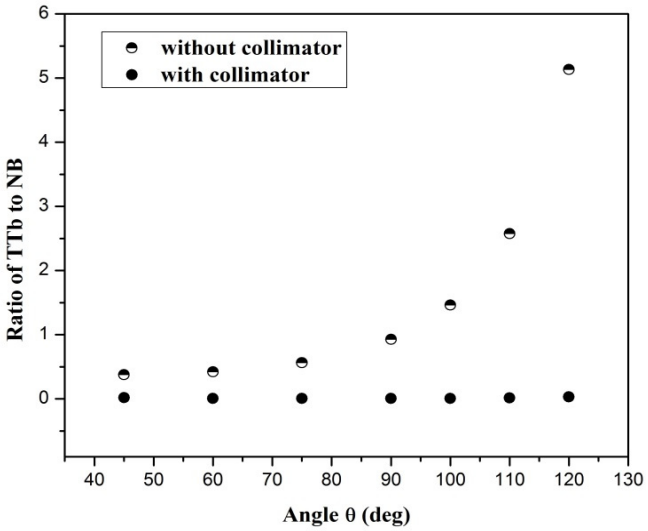

Figure 3. Model calculations of the ratio of total TTB background to the normal gas BS (NB) emitted from 4.0 keV electron collisions with free Argon atoms as a function of detection angle (θ) for a photon energy of 2.4 keV. The filled circles show the ratio of TTB to normal gas BS (NB) with use of a collimator while the half-filled circles show the same ratio without use of a collimator.

4. Data Analysis

A typical X-ray spectrum containing the characteristic Ar-K peak and the associated BS background produced from 4.0 keV electrons incident on free Ar atoms at a detection angle of 90° with respect to the electron beam direction is shown in Figure 4. The characteristic Ar-K peak is seen to consist of contributions from its Kα and Kβ lines. A shoulder of the Kβ lines is found on the right side of the main peak (Kα); there is also a weak shoulder on the left side whose origin could be possibly assigned to the weak forbidden channel M1 (2 s–1 s); however, it remains to be ascertained.

The X-ray spectra were recorded for photon emission angles of θ = 45°, 60°, 70°, 90°, 100°, 110° and 120° with respect to the electron beam direction. For obtaining DDCSs of argon BS, it was necessary to subtract the characteristic peaks appearing in the region between 2.3 keV and 3.2 keV of the X-ray spectra. The subtraction of the abovementioned three peaks from the recorded spectra was performed by employing a three peak Gaussian fitting procedure, see Figure 5. For this, we fitted the continuum background underneath the peaks by using a linear interpolation method, taking the data points from both sides of the three peaks.

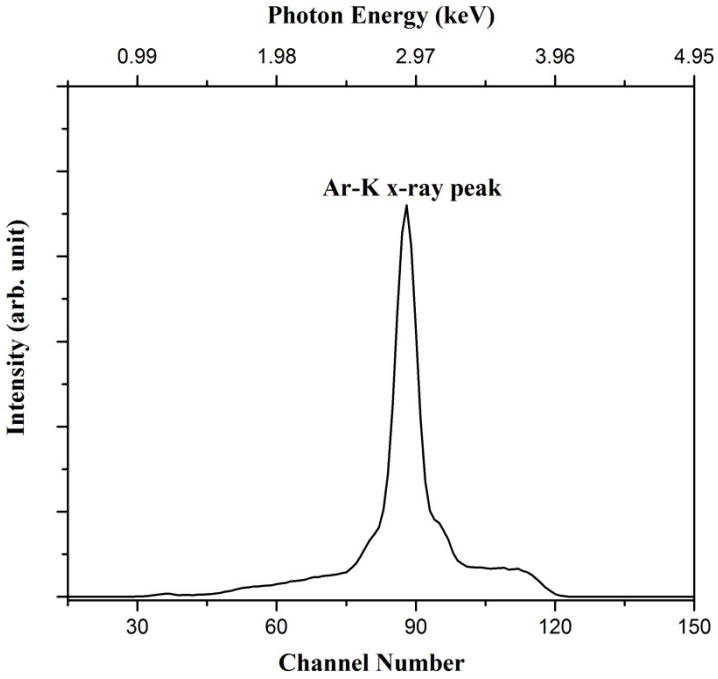

Figure 4. A typical X-ray spectrum showing the characteristic Ar-K peak at photon energy k = 2.92 keV and the continuous BS background produced from collisions of 4.0 keV electrons with free Ar atoms measured at emission angle of 90°. The top scale shown in the figure refers to the photon energy k.

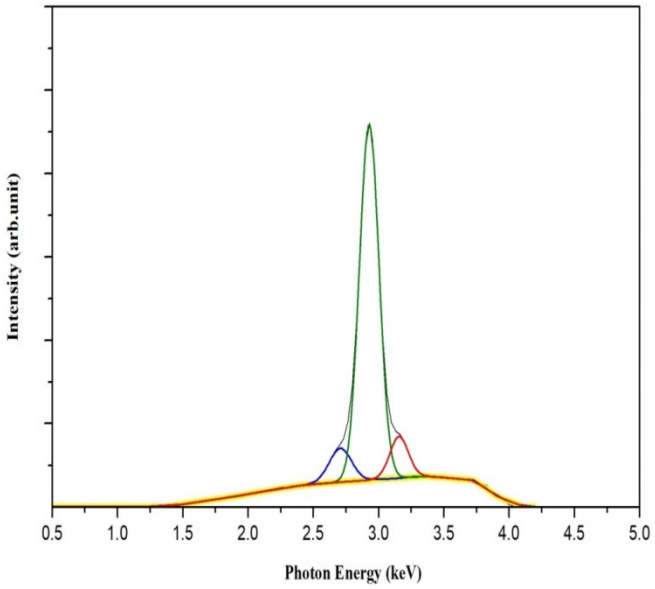

Figure 5. A typical X-ray spectrum showing the Gaussian peak fitting procedure. The green and the red curves show the Gaussian fits for Ar-K_α and K_β x-ray peaks, respectively; while the blue curve shows the fitting of the unidentified peak (as explained in the text). The yellow curve shows the contribution of bremsstrahlung in the photon energy region of 1.5–4.0 keV.

The experimental relative DDCSs of BS in units of the number of photons keV^{-1} $electron^{-1}$ sr^{-1} were obtained using the following relation:

$$DDCS = \frac{N_{BS}(k,\theta)}{N_e\, dk\, d\Omega\, \varepsilon(k)} \quad (1)$$

where N_{BS} (k,θ) is the number of BS photons of energy k emitted at an angle θ, N_e is the total number of incident electrons, $\varepsilon(k)$ is the efficiency of the detector for detecting BS photons of energy k. In order to put the relative DDCS data on *an absolute scale,* we have first determined a normalizing factor $F(K)$, as explained below in Equation (2); this factor is obtained by taking the ratio of detection efficiency $\varepsilon(K)$ of the detector at the photon energy of the Ar-K peak and the photon yield of the characteristic K X-ray peak. The BS yields at different photon energies (k) were obtained by integrating the photon counts in the energy window of Δk = 100 eV in the photon energy range between 2.0 keV and 3.6 keV. It may be mentioned here that the lowest photon energy in the present experiments was taken to be 2.0 keV mainly due to the small and less certain detection efficiency of the detector. The measured DDCS data of BS spectra were put on an absolute scale by using the following relation:

$$\frac{d^2\sigma(k,\theta)}{dkd\Omega} = F(K)\frac{\sigma_K\omega_K}{4\pi}\frac{N_{BS}(k,\theta)}{\varepsilon(k)\Delta k} \quad (2)$$

where $F(K) = \varepsilon(k)/N(K)$ is the normalizing factor, σ_K are *absolute* ionization cross section and ω_K fluorescence yield of Ar-K shell at a given impact energy, respectively; values of σ_K and ω_K have been taken from Tawara et al. [37], $d\Omega$ is the solid angle element of the detector subtended at the target, *N(K)* is the integrated K X-ray photon counts, $N_{BS}(k,\theta)$ represent the integrated BS photon counts in interval k and $k \pm \Delta k$ = 100 eV. The bremsstrahlung as well as the K X-ray photons were corrected for different absorption media, that is, air and hostaphan polyester foil.

Uncertainty in measurements of the reported results was determined by adding in quadrature different errors involved in X-ray absolute cross sections (~13%) [37], detection efficiency (~4%), TTB background corrections at extreme detection angles (4% and 6%) and statistical errors of photon counts in the BS (~6–8%) and K peaks (<1%), respectively. Thus, the total relative uncertainty of measurements is found to be about 16%.

5. Results and Discussion

5.1. Energy Distributions of BS Photons

The plots for the variation of measured absolute DDCSs of BS photons as a function of k in the range of 2.0–3.6 keV are shown at different emission angles, θ = 45°, 60°, 75°, 90°, 100°, 110° and 120° in Figure 6a–g, respectively. The measured data points are shown with relative uncertainty of16% by filled circles and they are compared with two theoretical calculations, namely, with KQP [10] and SA [28] predictions.

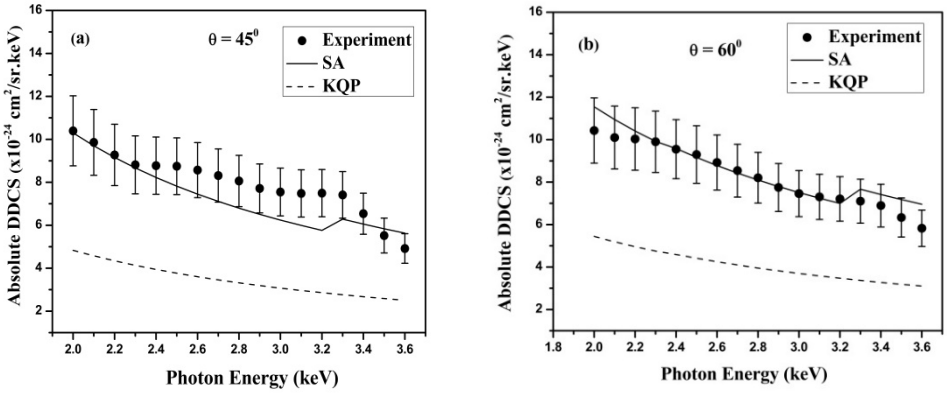

Figure 6. *Cont.*

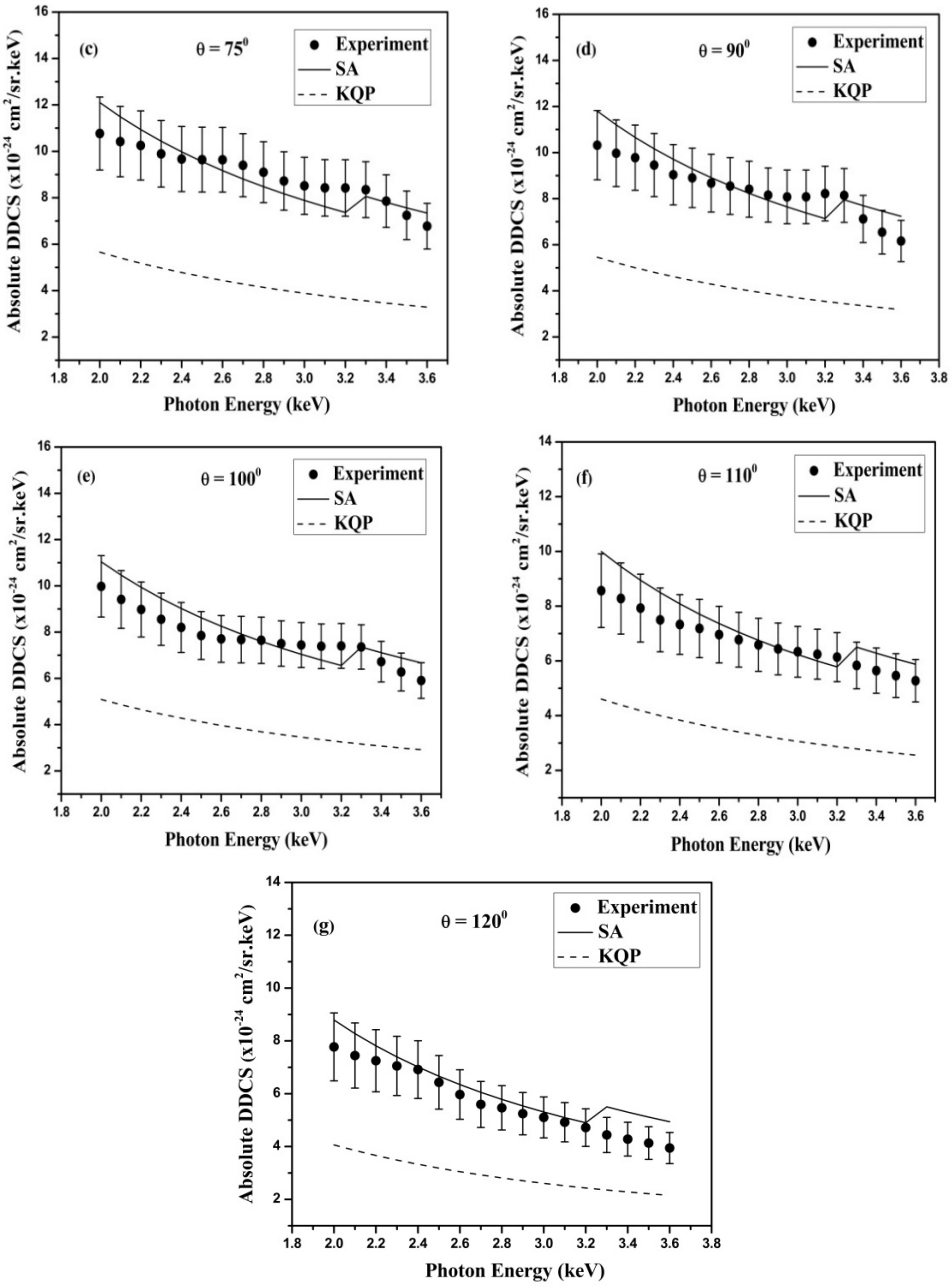

Figure 6. Comparison of experimental absolute DDCSs of BS photons emitted at θ = (**a**) 45°, (**b**) 60°, (**c**) 70°, (**d**) 90°, (**e**) 100°, (**f**) 110° and (**g**) 120° from 4.0 keV electrons interacting with free Ar atoms as a function of BS photon energy to the predictions of Kissel Quarles Pratt (KQP) [10] and Stripping Approximation (SA) [28] theories. Filled circles are experimental data points and dashed and solid line curves represent the calculations from KQP and SA theories, respectively.

A close examination of the results presented in Figure 6a–g reveals the following observations:

The predictions of KQP calculations are known to be valid for ordinary bremsstrahlung (OBS) radiation for free atoms and molecules or for extremely thin targets where each incident electron only interacts with a single target atom; the comparison of cross sections calculated by OBS theory and the present experimentally measured *absolute* cross sections exhibits a large discrepancy between them. In all the cases studied here, it is seen that the experimental *absolute* DDCSs are larger by an average factor of more than two compared to those predicted by KQP calculations. This discrepancy clearly suggests that there is a definite contribution of an additional type of bremsstrahlung, presumably, the polarization bremsstrahlung (PBS) to the OBS spectra. The experimental data are in overall good

agreement with the trends predicted by calculations using SA theory both in magnitude as well as in photon energy dependence within the uncertainty of measurements except for the data measured at $\theta = 120°$, for which the SA is seen to slightly overestimate the experiment for high energy photons. It must be mentioned here that the SA theory includes both OBS and PBS contributions, while KQP theory does not take into account any polarization component in the calculations.

The present results suggest that polarization bremsstrahlung not only contributes at the atomic resonance, that is, at Ar-K edge in the present case, but it also contributes to the total bremsstrahlung spectrum even at energies not associated with atomic resonance. This conclusion was also drawn by Portillo and Quarles [27] in their studies of the variation of photon energy and DDCSs as a function of the photon energy for Ne and Ar free atoms under the impact of 28 keV and 50 keV electrons.

The approximation of the angular distributions when calculating the SA by using the same angular distributions as that in OBS seems to be valid for our results too. This conclusion is favored most probably due to the success of reducing the TTB background to a minimum magnitude in our experiments.

The experimental data are found to become flatter and structureless with detection angles beyond $\theta = 100°$. Nevertheless, there is a satisfactory agreement between experiment and SA predictions for all angles and photon energies within the uncertainty of measurements, except the mismatch for $k = 3.3$–3.6 keV at $\theta = 120°$. This result further shows that the PBS contribution remains dominant over the OBS throughout the total spectrum.

The discrepancy observed between the experimental results and the SA predictionsh, especially for high energy photons measured at $\theta = 120°$, may arise due to the fact that the SA theory does not account for the terms arising from interference effects between the ordinary and the polarization bremsstrahlung processes. This point is expected to be resolved only after the appropriate calculations involving interference terms become available.

Experimental DDCS data are seen to overestimate slightly the SA calculations in the photon energy range between 2.4 keV and 3.3 keV when measured at $\theta = 45°$; however, this feature slowly reverses when going to higher values of θ. The above discrepancy arises most probably due to a critical passage of the electron beam near the collimator at the most forward angle, giving rise to some additional TTB background for all photon energies; however, this problem does not occur at larger angles. Nevertheless, the experimental data measured in the considered angular range are seen to be in reasonably good agreement with the SA calculations within the uncertainty of measurements.

Another feature of the experimentally measured data for photon energy distributions at $\theta = 120°$ is noted. This feature shows the similar trend of photon energy distribution, as is shown by the KQP calculations. This discrepancy between the measured data and the SA predictions is speculated due to non-inclusion of the interference effect between OBS and PBS which may result in a canceling out effect on the presence of atomic resonance in this region. In order to verify this effect, a new theoretical model is needed to develop.

The DDCS values of high-energy photons (3.6 keV) are found to reduce by a factor of about two with respect to that of the lowest energy photons, see, for example, Figure 6a–g; however, these values are still larger by a factor of about two with respect to the predictions made by KQP theory. A similar feature is also noted for the DDCS values measured at other detection angles.

In view of the above observations, it may be stated that there is a signature of PBS on top of the OBS in the total BS spectrum and that there is a contribution of the cross section of PBS, amounting to more than a factor of two compared to the OBS cross sections throughout the total X-ray spectrum. The energy dependence of PBS emitted from the Ar gaseous target under the impact of 4.0 keV electrons shows that PBS intensity also depends on the emission angle with respect to the incident electron beam direction and its distribution is photon energy dependent. There is also a weak signature of atomic resonance structure at the Ar-K edge in the reported results associated with a large uncertainty. This large uncertainty of measurements mainly arises on account of large uncertainty involved in the absolute X-ray cross sections of the Ar-K shell, which is reported to be 13% [36], as mentioned earlier in Section 2.

5.2. Angular Dependence of BS Photons

Angular distributions of the relative intensity of total BS photons measured at emission angle θ with respect to the intensity measured at θ = 90°, i.e., I(θ)/I(90°), produced in collisions of 4.0 keV electrons with free Ar atoms, have been studied. For comparison of the measured angular distributions of BS photons of different energies with those of theoretical predictions, we have chosen to plot the angular distributions for BS photons with energies of 2.0 keV, 2.2 keV, 2.4 keV, 2.5 keV, 2.8 keV, 3.2 keV, 3.4 keV and 3.6 keV in Figure 7a–h, respectively.

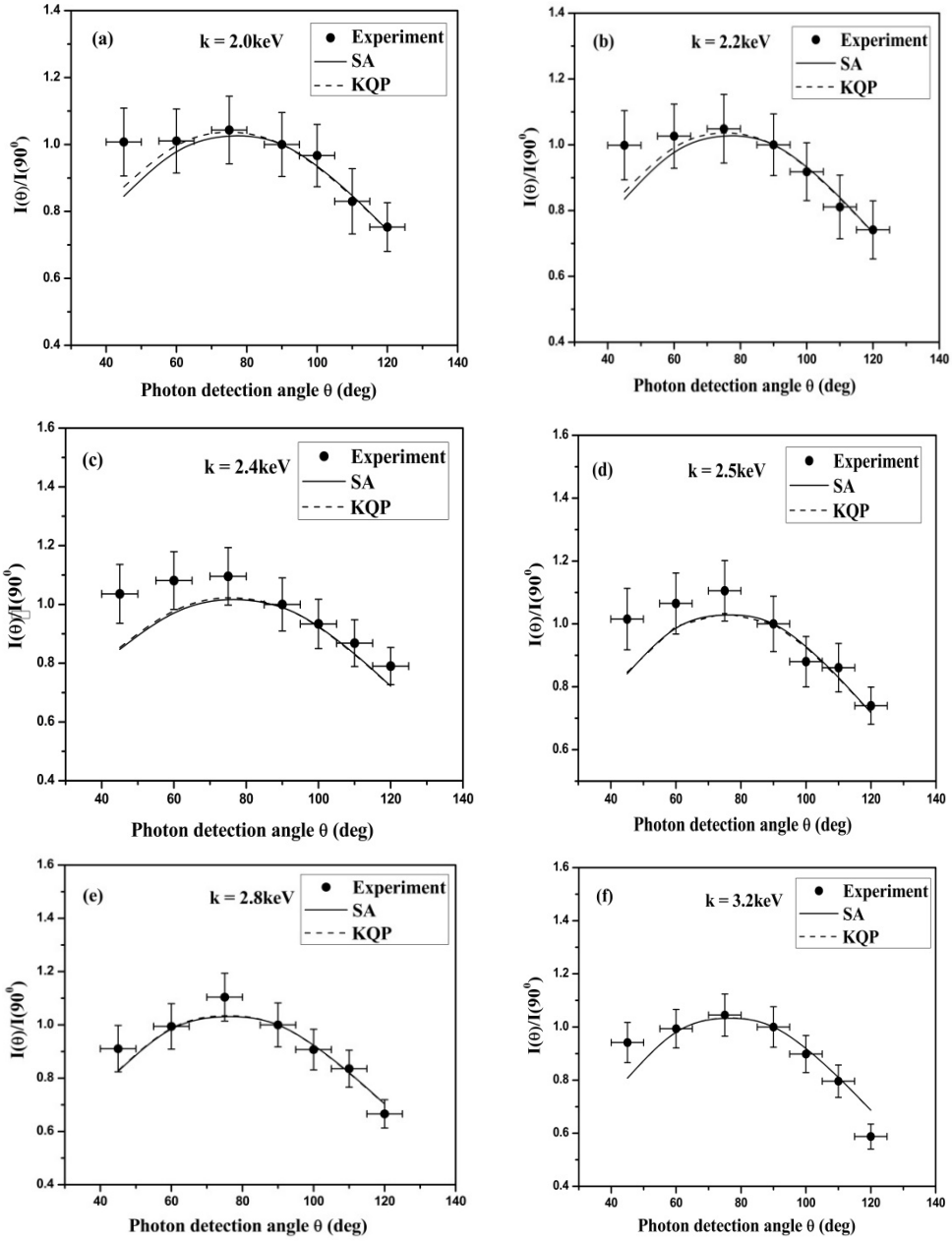

Figure 7. *Cont.*

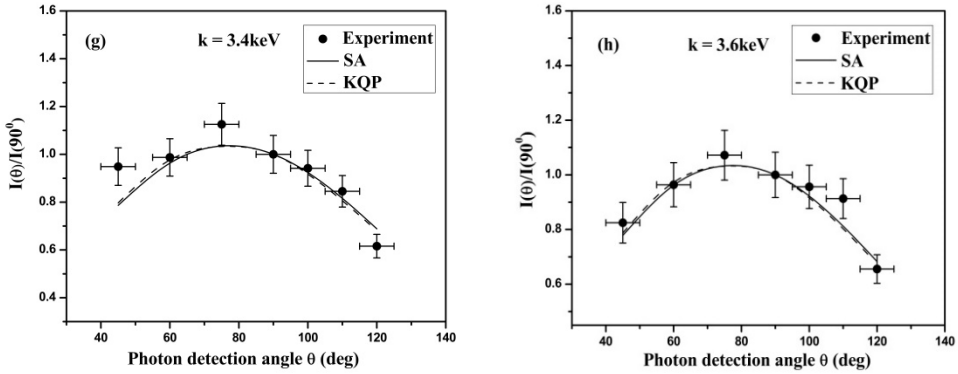

Figure 7. Angular distributions of the relative intensity of BS photons with energies of (**a**) 2.0 keV, (**b**) 2.2 keV, (**c**) 2.4 keV, (**d**) 2.5 keV, (**e**) 2.8 keV, (**f**) 3.2 keV, (**g**) 3.4 keV and (**h**) 3.6 keV under impact of 4.0 keV electrons with free Ar atoms. The solid curves denote the SA [28] calculations, while the dashed curves represent the KQP [10] predictions. The filled circles are the experimental data points shown with horizontal and vertical error bars, indicating uncertainties in angle and in relative intensity, respectively.

In the above plots, the vertical and the horizontal error bars shown on the experimental data points represent the total uncertainty in relative intensity (8–10%) and in measured angle (3%), respectively. It is noted that for all considered photon energies, the intensity attains a maximum value around $\theta = 72°$. However, it is further seen that in each plot, the photons are emitted anisotropically, with their lower minimum intensity in the backward direction. Furthermore, there is a noticeable difference in shape of the angular distributions obtained from experiment and theory; both theories (KQP and SA) are seen to underestimate the experiment at forward angles for low-energy photons. Since these plots are made for an intensity ratio of a photon of known energy measured at a given emission angle, the detector efficiency plays no role in this ratio. However, the discrepancy of about 15% existing between the experiment and theories for most forward angles probably arises due to a critical passage of the electron beam near the collimator, giving rise to some TTB background (see, for example, Figures 5 and 6a). One noticeable feature of the angular distributions of the BS radiation studied here is that both the KQP and the SA theories exhibit a similar shape of the angular distributions; this is understood to be due to the fact that the PBS has a simple dipole shape function which is very close to what KQP has used at these low energies. The good agreement of these theories with the experimental data for angular distributions is an indication of the significant reduction in the TTB background.

In light of the above observations and discussion, it may be stated with some confidence that there is a definite contribution of the PBS to the total BS spectrum with a significant magnitude over OBS; also, there is a weak signature of the atomic resonance structure at the Ar-K edge in the reported results.

6. Conclusions

We have presented new results for measurements of the absolute double differential cross sections (DDCSs) of BS photons emitted from 4.0 keV electrons incident on free Ar atoms in an angular detection range of 45°–120°. A significant reduction of thick target bremsstrahlung (TTB) generated from the chamber walls and from the photon transmission windows have been achieved by modifying the experimental set-up used previously. The results of photon energy distributions measured at different detection angles and the angular distributions of photons of a given energy have been compared with theoretical predictions using Kissel–Quarles–Pratt (KQP) tabulations for ordinary bremsstrahlung (OBS) and employing stripping approximation (SA) for total bremsstrahlung including polarization bremsstrahlung (PBS). A satisfactory agreement between experiment and SA theory for absolute DDCSs of bremsstrahlung provides convincing evidence for the contribution of polarization bremsstrahlung at the considered impact energy of electrons on one hand, while on the other hand, it exhibits an appreciable discrepancy (about a factor of two) between the experiment and the KQP predictions

for photon energy distributions at all detection angles measured in these experiments. In addition, the present results of the angular dependence of photons of different energies show anisotropic distributions and they are shown to be in reasonable agreement with both theories except for photons of low energies. Good agreement for the angular distributions with both theoretical predictions is a further indication of a significant reduction in the background produced from TTB bremsstrahlung processes; this conclusion is also supported by the results of our model calculations for the ratio of total TTB background to the normal BS spectrum. The relative importance of polarization bremsstrahlung and ordinary bremsstrahlung is recognized from the fact that, in a number of cases, it is almost not possible to visualize the correct picture of bremsstrahlung without considering the electronic structure of the target atom. When polarization bremsstrahlung and ordinary bremsstrahlung are taken simultaneously and added up, it becomes feasible to explain easily the results that were not contained in the earlier theories of bremsstrahlung which actually relied on a shielding approximation that normally ceases to occur in long-range collisions.

Author Contributions: Formal analysis, S.P. and B.S.; Investigation, S.P. and B.S.; Methodology, S.P. and R.S.; Software, C.A.Q.; Supervision, R.S.; Writing—original draft, S.P. and R.S.; Writing—review and editing, B.S., S.K., B.K.S., C.A.Q. and R.S. All authors have read and agreed to the published version of the manuscript.

Funding: The work presented in this paper has been supported by the Science and Engineering Research Board (SERB), a division of the Department of Science and Technology (DST), Government of India under research project No.: SR/S2/LOP-033/2012.

Acknowledgments: S. Prajapati, S. Kumar and B. Singh are grateful to the University Grants Commission (UGC), New Delhi, Government of India and the Banaras Hindu University for providing the research fellowships during the execution of this work.

Conflicts of Interest: Authors declare no conflict of interest.

References

1. Hippler, R.; Saeed, K.; McGregor, I.; Kleinpoppen, H.Z. Dependence of Bremsstrahlung Radiation from Free Atoms. *Phys. Rev. Lett.* **1981**, *46*, 1622–1625. [CrossRef]
2. Hippler, R.; Saeed, K.; McGregor, I.; Kleinpoppen, H. Energy dependence of characteristic and bremsstrahlung cross sections of argon induced by electron bombardment at low energies. *Zeitschrift für Phys. A Atoms Nucl.* **1982**, *307*, 83–87. [CrossRef]
3. Quarles, C.A.; Heroy, D.B. Atomic-field bremsstrahlung from 50-140-keV electrons. *Phys. Rev. A* **1981**, *24*, 48–54. [CrossRef]
4. Estep, L.; Quarles, C.A. Atomic-field bremsstrahlung from hydrogen, helium, nitrogen and neon from 5 to 15 keV. *Phys. B+C* **1987**, *145*, 369–376. [CrossRef]
5. Semaan, M.; Quarles, C. Bremsstrahlung spectrum from low-energy-electron bombardment of rare-gas atoms. *Phys. Rev. A* **1981**, *24*, 2280–2283. [CrossRef]
6. Semaan, M.; Quarles, C. Z dependence of atomic-field bremsstrahlung. *Phys. Rev. A* **1982**, *26*, 3152–3154. [CrossRef]
7. Tseng, H.K.; Pratt, R.H. Exact Screened Calculations of Atomic-Field Bremsstrahlung. *Phys. Rev. A* **1971**, *3*, 100–115. [CrossRef]
8. Tseng, H.K.; Pratt, R.H.; Lee, C.M. Electron bremsstrahlung angular distributions in the 1–500 keV energy range. *Phys. Rev. A* **1979**, *19*, 187–195. [CrossRef]
9. Quarles, C.; Estep, L. Molecular-field bremsstrahlung in ethane, ethene and ethyne. *Phys. Lett. A* **1986**, *114*, 9–12. [CrossRef]
10. Kissel, L.; Quarles, C.A.; Pratt, R.H. Shape functions for atomic-field bremsstrahlung from electrons of kinetic energy 1–500 keV on selected neutral atoms $1 \leq Z \leq 92$. *At. Data Nucl. Data Tables* **1983**, *28*, 381–460. [CrossRef]
11. Buimistrov, V.M.; Trakhtenberg, L.I. Bremsstrahlung cross section in scattering of an electron by a Hydrogen Atom. *JETP* **1976**, *42*, 54–57.
12. Verkhovtseva, E.T.; Gnatchenko, E.V.; Pogrebnjak, P.S. Investigation of the connection between "giant" resonances and "atomic" bremsstrahlung. *J. Phys. B At. Mol. Phys.* **1983**, *16*, L613–L616. [CrossRef]

13. Korol, A.V.; Lyalin, A.G.; Solovy'ov, A.V. Total bremsstrahlung spectra of 1–25 keV electrons on Ne and Ar. *J. Phys. B At. Mol. Opt. Phys.* **1997**, *30*, L115–L121. [CrossRef]
14. Korol, A.V.; Obolensky, O.I.; Solov'yov, A.V.; Solovjev, I.A. The full relativistic description of the bremsstrahlung process in a charged particle-atom collision. *J. Phys. B At. Mol. Opt. Phys.* **2001**, *34*, 1589–1617. [CrossRef]
15. Korol, A.V.; Lyalin, A.G.; Obolensky, O.I.; Solovyov, A.V.; Solovjev, I.A. A relativistic description of the polarization mechanism of elastic bremsstrahlung. *J. Exp. Theor. Phys.* **2002**, *94*, 704–719. [CrossRef]
16. Yamabe, C.; Buckman, S.J.; Phelps, A.V. Measurement of free-free emission from low-energy-electron collisions with Ar. *Phys. Rev. A* **1983**, *27*, 1345–1352. [CrossRef]
17. Gurevich, A.V.; Valdivia, J.A.; Milikh, G.M.; Papadopoulos, K. Runaway electrons in the atmosphere in the presence of a magnetic field. *Radio Sci.* **1996**, *31*, 1541–1554. [CrossRef]
18. Chen, Y.; Wu, Z.; Gao, W.; Ti, A.; Zhang, L.; Jie, Y.; Zhang, J.; Huang, J.; Xu, Z.; Zhao, J. Application of visible bremsstrahlung to Z eff measurement on the Experimental Advanced Superconducting Tokamak. *Rev. Sci. Instrum.* **2015**, *86*, 023509. [CrossRef]
19. Yerokhin, V.A.; Surzhykov, A. Electron-atom bremsstrahlung: Double-differential cross section and polarization correlations. *Phys. Rev. A* **2010**, *82*, 062702. [CrossRef]
20. Mangiarotti, A.; Jakubassa-Amundsen, D.H. Higher-order theories for relativistic electron-atom bremsstrahlung in comparison with experiment. *Phys. Rev. A* **2017**, *96*, 042701. [CrossRef]
21. Quarles, C.A.; Portillo, S. Review of absolute doubly differential cross-section experiments and cross-section ratios for electron bremsstrahlung from rare gas atom and thin-film targets. *Radiat. Phys. Chem.* **2006**, *75*, 1187–1200. [CrossRef]
22. Ishii, K. Continuous X-rays produced in light-ion–atom collisions. *Radiat. Phys. Chem.* **2006**, *75*, 1135–1163. [CrossRef]
23. Ishii, K.; Morita, S. Continuum x rays produced by light-ion—Atom collisions. *Phys. Rev. A* **1984**, *30*, 2278–2286. [CrossRef]
24. Ishii, K.; Morita, S.; Tawara, H. Bremsstrahlung induced by proton and He-ion bombardments in the 1–4-Mev/amu energy range. *Phys. Rev. A* **1976**, *13*, 131–138. [CrossRef]
25. Ishii, K.; Morita, S. Atomic bremsstrahlung produced by heavy-ion bombardments. *Phys. Rev. A* **1985**, *31*, 1168–1170. [CrossRef]
26. Salvat, F.; Fernandez-Varea, J.M.; Sempau, J. *P ENELOPE—A Code System for Monte Carlo Simulation of Electron and Photon Transport*; OECD/NEA Data Bank/NSC Doc; OECD: Paris, France, 2015.
27. Portillo, S.; Quarles, C.A. Absolute Doubly Differential Cross Sections for Electron Bremsstrahlung from Rare Gas Atoms at 28 and 50 keV. *Phys. Rev. Lett.* **2003**, *91*, 173201. [CrossRef] [PubMed]
28. Avdonina, N.B.; Pratt, R.H. Bremsstrahlung spectra from atoms and ions at low relativistic energies. *J. Phys. B At. Mol. Opt. Phys.* **1999**, *32*, 4261–4276. [CrossRef]
29. Requena, S.; Williams, S.; Quarles, C.A. A comparison of the bremsstrahlung yields from 53keV electrons on gold targets produced by PENELOPE and experiment. *Nucl. Instrum. Methods Phys. Res. Sect. B Beam Interact. Mater. Atoms* **2010**, *268*, 3561–3563. [CrossRef]
30. Requena, S.; Gonzales, D.; Williams, S. Angular dependence of bremsstrahlung produced by 17.5-keV electrons incident on thick Ag. *Phys. Rev. A* **2011**, *83*, 022712. [CrossRef]
31. Ambrose, R.; Kahler, D.L.; Lehtihet, H.E.; Quarles, C.A. Angular dependence of thick-target bremsstrahlung. *Nucl. Instrum. Methods Phys. Res. Sect. B Beam Interact. Mater. Atoms* **1991**, *56–57*, 327–329. [CrossRef]
32. Aydinol, M.; Hippler, R.; McGregor, I.; Kleinpoppen, H. Angular distribution of X-radiation following electron bombardment of free atoms. *J. Phys. B At. Mol. Phys.* **1980**, *13*, 989–998. [CrossRef]
33. Yadav, N.; Bhatt, P.; Singh, R.; Singh, B.K.; Quarles, C.A.; Shanker, R. An apparatus to study the energy and angular distributions of electron-bremsstrahlung photons from gaseous targets. *Radiat. Phys. Chem.* **2014**, *97*, 25–30. [CrossRef]
34. Astapenko, V.A. Bremsstrahlung of relativistic electron scattering on an atom: Comparison of various channels. *Phys. Lett. Sect. A Gen. At. Solid State Phys.* **2007**, *361*, 242–247. [CrossRef]
35. Quarles, C.A. *Accelerator-Based Atomic Physics: Techniques and Applications*; Shafroth, S.M., Austin, J.C., Eds.; AIP Press: Woodbury, NY, USA, 1997; ISBN 1563964848.

36. Semaan, M.; Quarles, C.A. A model for low-energy thick-target bremsstrahlung produced in a scanning electron microscope. *X-ray Spectrom.* **2001**, *30*, 37–43. [CrossRef]
37. Tawara, H.; Harrison, K.G.; De Heer, F.J. X-ray emission cross sections and fluorescence yields for light atoms and molecules by electron impact. *Physica* **1973**, *63*, 351–367. [CrossRef]